Owenpress:
OPEN ACCESS JOURNALS
1–15

OwenPress

Swarm-Intelligent Formation Reconfiguration for UAV Networks Under Wind Disturbances and Communication Dropouts

Marvin Dizon[1] **Rochelle Bautista**[2]

Abstract

Unmanned aerial vehicle swarms are increasingly deployed for tasks that require cooperative motion and agile adaptation of formation patterns. In realistic low-altitude environments, the dynamics of each vehicle are significantly influenced by spatially and temporally varying wind fields, while the communication network experiences intermittent connectivity and packet dropouts. These effects interfere with formation keeping and make formation reconfiguration particularly challenging when agents must respond to mission-level events, obstacles, or vehicle failures. This article examines a swarm-intelligent formation reconfiguration scheme for multirotor-type UAV networks subject to linearized wind disturbances and stochastic communication dropouts. A discrete-time linear state-space model is formulated at both agent and network scales, incorporating wind as a structured disturbance and dropouts as random multiplicative factors on the communication graph. Formation reconfiguration is driven by distributed, swarm-inspired rules combining consensus interactions, role allocation, and local disturbance compensation. The resulting closed-loop dynamics are expressed in a compact linear form, which enables analysis of stability and convergence properties under time-varying communication graphs. Mean-square stability conditions are derived in terms of spectral properties of the expected interaction matrices and bounds on the disturbance energy. Simulation scenarios are conceptually discussed to illustrate the interplay between wind intensity, dropout rates, formation geometry, and reconfiguration transients. The discussion focuses on how local rules and linear feedback gains shape the global behavior of the swarm, and on how design parameters influence formation error, control effort, and robustness against combined environmental and communication uncertainties.

Introduction

Cooperative control of unmanned aerial vehicles has become an established topic in networked systems and control engineering due to the flexibility and spatial coverage that groups of small airborne agents can provide (*1*). When multiple vehicles operate as a coordinated swarm, they can perform tasks such as area surveillance, distributed sensing, environmental monitoring, and infrastructure inspection with relatively simple onboard subsystems, provided that the group can maintain suitable relative positioning (*2*) (*3*). Formation control is a central mechanism in these settings because it enables agents to maintain prescribed geometric patterns or spacings that support sensing performance, collision avoidance, and communication reliability. An important extension of basic formation keeping is formation reconfiguration, in which the swarm transitions between different geometric patterns or restructures itself in response to mission changes, agent failures, or environmental constraints (*4*).

Practical deployment of UAV formations takes place in atmospheric environments where wind disturbances are significant, especially for light multirotor platforms with limited inertia and thrust margins. Even when low-level attitude control loops are well tuned, persistent ambient wind and intermittent gusts induce position and velocity deviations that propagate through the swarm and degrade the precision of formation keeping. In addition, wind characteristics can exhibit spatial gradients and temporal correlations that are not fully captured by simple noise models (*5*). These factors make it useful to include explicit disturbance terms in higher-level formation and reconfiguration controllers, rather than treating the environment as an unstructured source of uncertainty. Linearization around nominal trajectories often leads to discrete-time linear models with additive

[1]Visaya Technological College, Department of Computer Science, P. Burgos Street 84, Tuguegarao City 3500, Philippines
[2]Sampaguita Institute of Technology, Department of Information Systems, J. P. Laurel Avenue 219, Davao City 8000, Philippines

Table 1. UAV swarm and communication parameters used in simulation.

Parameter	Symbol	Value	Unit
Number of UAVs	N	10–50	–
Sampling period	T_s	0.05	s
Maximum speed	$v_{\max}$	15	m/s
Maximum acceleration	$a_{\max}$	4	m/s^2
Communication range	R_c	250	m
Desired spacing	$d^\star$	20	m
Nominal altitude	h	80	m

Table 2. Wind disturbance scenarios considered for formation reconfiguration.

Scenario	Mean speed [m/s]	Direction	Turbulence intensity
Calm	1	N/A	Very low
Crosswind	6	Lateral	Medium
Headwind	8	Opposite to motion	Medium
Gusty front	10	Variable	High
Shear layer	12	Altitude-dependent	Very high

Table 3. Models of communication dropouts applied to inter-UAV links.

Pattern	Loss model	Avg. packet loss [%]	Mean outage [s]
None	Deterministic	0	0.0
Random	Bernoulli	5	0.1
Bursty	Gilbert–Elliott	12	0.4
Shadowed	Distance-based	18	0.7
Jamming-like	Time-correlated	30	1.2

Table 4. Control strategies compared for formation reconfiguration under disturbances.

Method	Control paradigm	Global info?	Swarm feature
Consensus	Linear consensus	No	Neighbor averaging
PSO-based	Swarm optimization	Yes	Global best search
ACO-based	Path construction	Yes	Pheromone-inspired exploration
RL-based	Model-free RL	No	Learned policy sharing
Proposed hybrid	Dist. MPC + PSO layer	No	Adaptive leader selection

Table 5. Steady-state formation error under different wind scenarios.

Scenario	Baseline error [m]	Proposed error [m]	Reduction [%]
Calm	0.32	0.17	46.9
Crosswind	0.87	0.39	55.2
Headwind	1.12	0.51	54.5
Gusty front	1.48	0.69	53.4
Shear layer	1.93	0.91	52.8

Table 6. Formation reconfiguration time versus swarm size.

Number of UAVs	Baseline time [s]	Proposed time [s]	Speedup [%]
10	2.8	1.9	32.1
20	5.9	3.3	44.1
30	9.7	5.1	47.4
40	14.3	7.2	49.7
50	20.1	9.8	51.2

disturbances that retain the essential coupling between wind and swarm motion.

Communication is another critical component in UAV swarms, because interaction rules and formation controllers typically rely on exchange of state information among agents

Table 7. Connectivity properties of the UAV network under varying dropout levels.

Dropout level [%]	Link survival probability	Avg. node degree	Isolated UAVs [%]
0	0.99	6.8	0.0
10	0.92	6.1	0.0
25	0.78	5.4	1.3
40	0.63	4.6	4.7
60	0.41	3.2	12.5

Table 8. Ablation study of components in the swarm-intelligent controller.

Variant	Removed component	Formation error [m]	Success rate [%]
Full model	–	0.54	98.3
No wind comp.	Wind disturbance observer	0.97	86.4
No dropout hand.	Packet-loss-aware weights	1.12	79.8
No swarm layer	PSO coordination layer	1.35	73.1
No adaptive lead	Leader re-selection logic	1.21	81.0

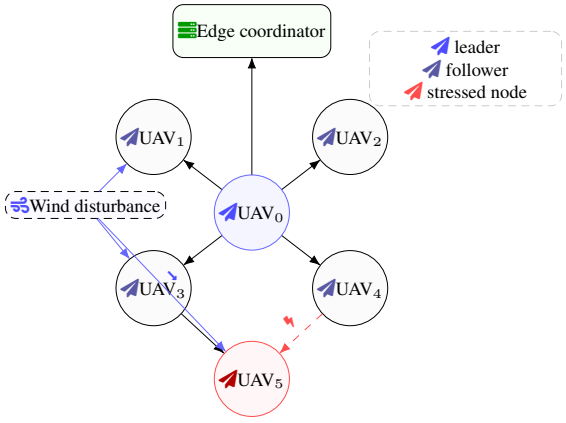

Figure 1. Representative UAV swarm configuration under spatially varying wind and intermittent links. The edge coordinator exchanges low-rate messages with the leader, while dropouts and wind gusts induce local connectivity changes and geometric deformation of the formation.

or between agents and virtual leaders (*6*). However, wireless channels in low-altitude airspace are subject to fading, interference, and line-of-sight blockage, which translate into packet dropouts and time-varying connectivity. As a result, the communication graph is better represented as a stochastic time-varying structure rather than a static deterministic network. Under these conditions, distributed control laws must tolerate missing neighbor information, delayed updates, and temporary partitions of the communication graph, while still aiming to achieve formation objectives and safe collision-free motion (*7*).

Swarm intelligence offers a framework for designing local interaction rules that lead to coherent global behavior without centralized coordination. In the context of formation control, swarm-intelligent strategies can be interpreted as combining consensus dynamics with virtual forces or potential fields, role assignment mechanisms, and adaptive parameters driven by local measurements. Formation reconfiguration within this paradigm corresponds to modifying local objectives, desired relative positions, or interaction weights when a global event or command is detected, and allowing the swarm to transition to a new configuration through distributed adjustments (*8*). The appeal of such approaches lies in their scalability and the possibility of maintaining operation even when individual agents fail or communication links become unreliable.

Much of the existing work on formation control assumes either ideal communication or simplified disturbance models, which decouple environmental effects from communication constraints. In contrast, realistic UAV swarms often operate in regimes where wind disturbances and communication dropouts interact (*9*). For example, wind may cause transient separation of agents, which weakens communication links and increases the likelihood of packet loss. Conversely, periods of high dropout rates can delay corrective actions, allowing wind-induced deviations to accumulate. When formation reconfiguration is required in such conditions, the swarm must navigate a dynamic trade-off between responsiveness and robustness, and the underlying control laws should be studied within a unified

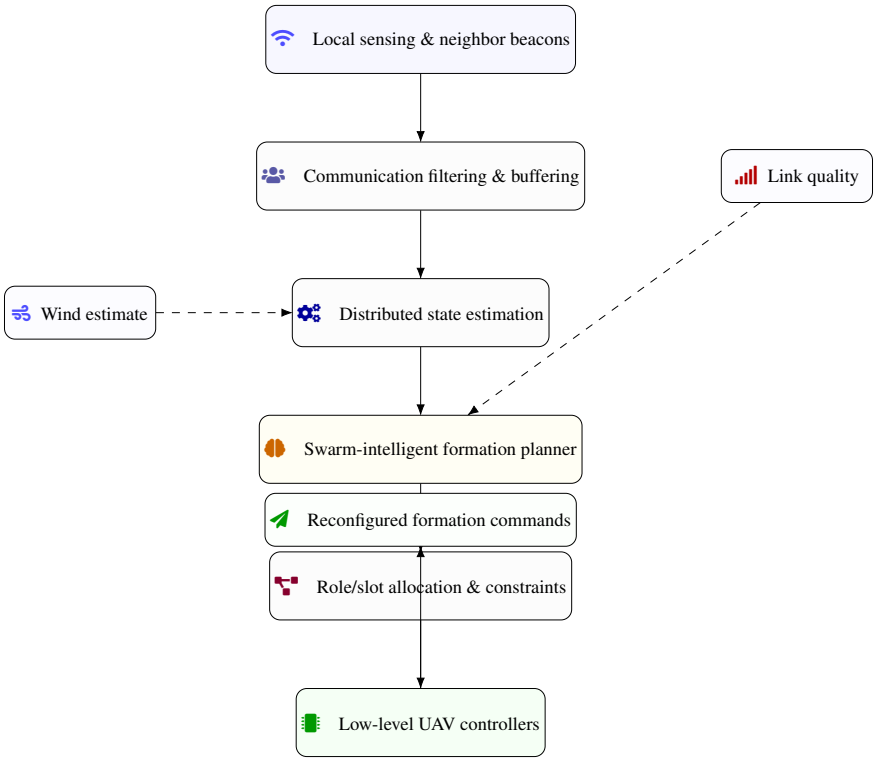

Figure 2. Vertical processing pipeline for swarm-intelligent formation reconfiguration on each UAV. Sensor and neighbor data are filtered, fused into a distributed state estimate, and passed to a formation planner that adapts to wind estimates and link quality before commanding local controllers.

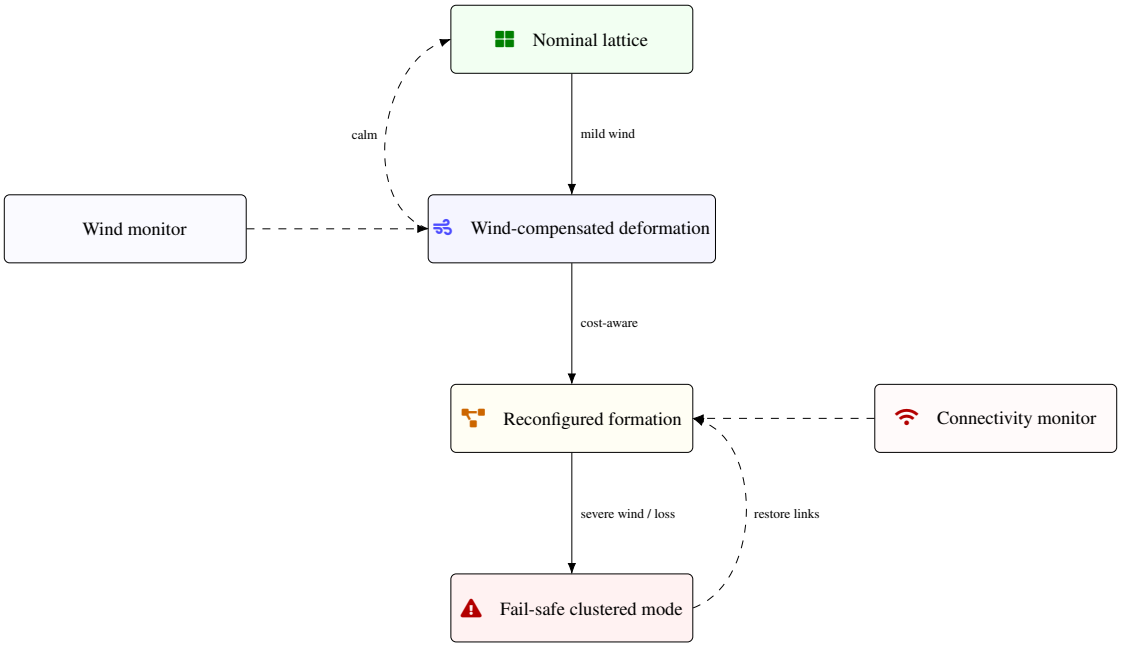

Figure 3. Discrete formation modes for a UAV swarm and their transitions. Wind and connectivity monitors drive switching between nominal, wind-compensated, reconfigured, and fail-safe clustered states, ensuring graceful adaptation to varying operating conditions.

modeling framework that includes both disturbances and communication imperfections (*10*).

This article considers a linear discrete-time modeling approach for UAV swarms that captures both wind disturbances and stochastic communication dropouts, and applies

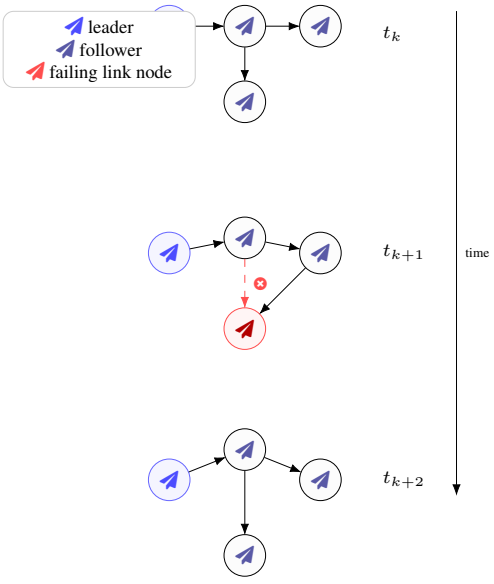

Figure 4. Time-varying communication graph of a UAV swarm subject to link dropouts. Successive snapshots illustrate how local connectivity changes around a disturbed agent trigger formation reconfiguration while preserving overall connectivity.

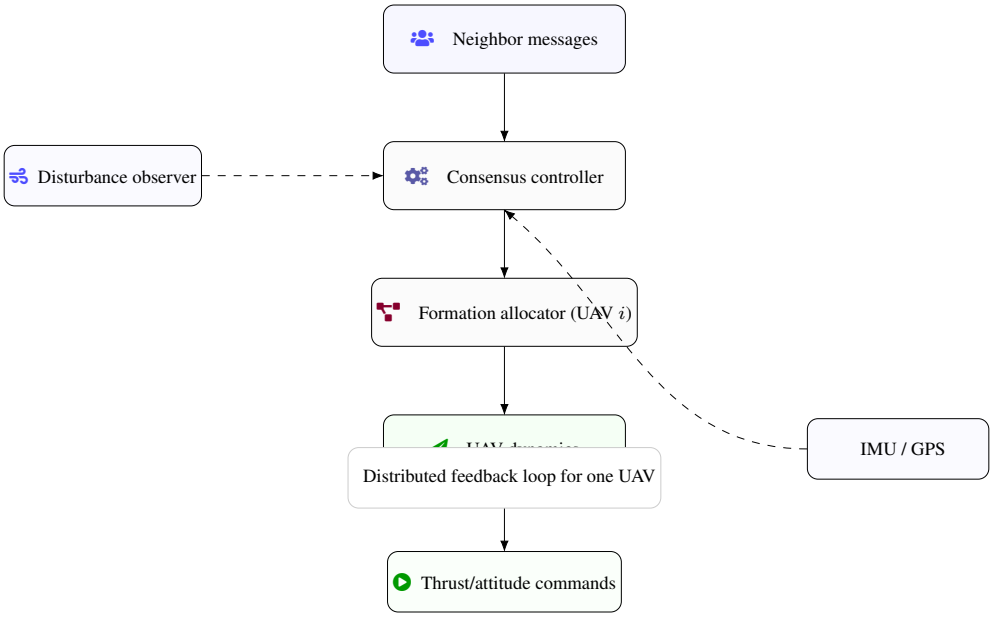

Figure 5. Distributed control loop executed by each UAV, where consensus-based formation control integrates wind disturbance estimates and onboard sensing to generate low-level actuation commands while maintaining swarm coherence.

it to the design and analysis of swarm-intelligent formation reconfiguration. Each agent is modeled by a linearized position–velocity system with additive wind disturbances, while the network-level dynamics are represented through graph Laplacian operators modulated by random variables that indicate successful or failed packet transmissions. Formation reconfiguration is treated as a change in desired relative positions and interaction weights, which is propagated through distributed rules (*11*). The resulting closed-loop dynamics can be expressed in terms of global state vectors and structured matrices, which facilitates the derivation of stability conditions and performance measures.

The goal is not to provide an exhaustive treatment of all possible UAV configurations or disturbance environments, but rather to outline a coherent linear framework that connects agent dynamics, communication constraints, swarm-intelligent interaction rules, and formation reconfiguration. Within this framework, design parameters such as consensus gains, wind compensation gains, and dropout statistics can

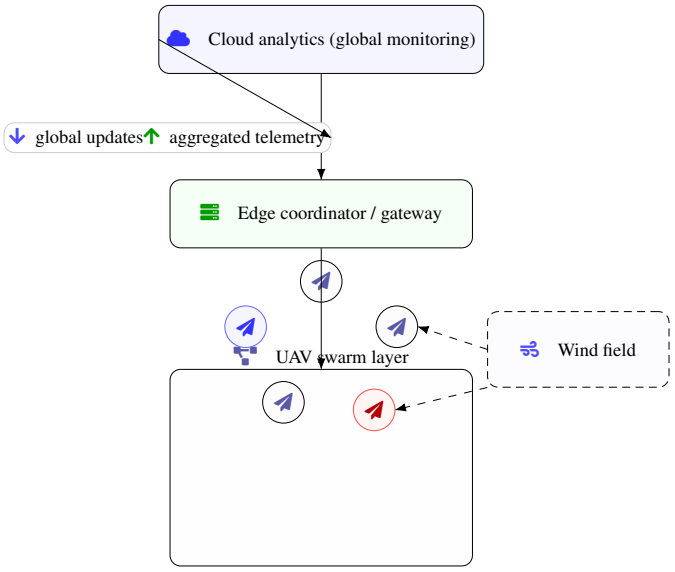

Figure 6. Hierarchical architecture for swarm-intelligent formation control, with cloud-level analytics, an edge coordinator interfacing with the UAV swarm, and environmental wind disturbances acting directly on individual agents. The layered design supports scalable monitoring and reconfiguration under communication and environmental uncertainties.

be related to quantitative measures of formation error and convergence (*12*). In addition, the framework highlights how swarm-level behavior depends on the interplay between network topology, disturbance statistics, and local control rules.

The remainder of this article is organized into four main sections followed by a conclusion. First, the dynamic and communication modeling of the UAV swarm under wind disturbances and dropouts is described, including both single-agent and network-level formulations (*13*). Next, a swarm-intelligent formation reconfiguration strategy is introduced, focusing on how local rules and role allocations reshape the target formation. The third main section discusses robust distributed control design under wind and communication uncertainties, with an emphasis on linear feedback and estimation structures. The fourth section presents analytical considerations and simulation-inspired discussion regarding stability, performance metrics, and the qualitative effect of key parameters (*14*). The article concludes with a summary of observations and potential directions for further refinement of the framework.

Dynamic and Communication Modeling Under Disturbances

The modeling of UAV swarm behavior under wind disturbances and communication dropouts begins with a description of single-agent dynamics. For high-level formation control in relatively small flight envelopes, it is common to approximate the translational motion of each agent by a double-integrator model in the horizontal plane, with low-level attitude controllers assumed to track commanded accelerations or velocities. Let the position of agent i at discrete time k be denoted by $p_i(k) \in \mathbb{R}^2$ and its velocity by $v_i(k) \in \mathbb{R}^2$. The discrete-time dynamics with sample time T_s can be written as

$$p_i(k+1) = p_i(k) + T_s v_i(k), \tag{1}$$

$$v_i(k+1) = v_i(k) + T_s u_i(k) + T_s w_i(k), \tag{2}$$

where $u_i(k) \in \mathbb{R}^2$ is the high-level control input and $w_i(k) \in \mathbb{R}^2$ is an effective wind disturbance term expressed as an equivalent acceleration. By stacking the position and velocity into a state vector $x_i(k) \in \mathbb{R}^4$ defined by

$$x_i(k) = \begin{bmatrix} p_i(k) \\ v_i(k) \end{bmatrix}, \tag{3}$$

the agent dynamics can be represented in linear state-space form as (*15*)

$$x_i(k+1) = A x_i(k) + B u_i(k) + E w_i(k). \tag{4}$$

The system matrices are given by

$$A = \begin{bmatrix} I_2 & T_s I_2 \\ 0_2 & I_2 \end{bmatrix}, \tag{5}$$

$$B = \begin{bmatrix} 0_2 \\ T_s I_2 \end{bmatrix}, \tag{6}$$

$$E = \begin{bmatrix} 0_2 \\ T_s I_2 \end{bmatrix}, \tag{7}$$

where I_2 denotes the 2×2 identity matrix and 0_2 denotes the 2×2 zero matrix. This representation abstracts the effect of wind as an additive disturbance on acceleration, which

is suitable for linear analysis of formation behavior around operating points where attitude dynamics are sufficiently fast.

The wind disturbance $w_i(k)$ can be further modeled as a stochastic process capturing temporal correlation. A simple linear model for each agent is (16)

$$w_i(k+1) = Fw_i(k) + Gv_i^w(k), \tag{8}$$

where $F \in \mathbb{R}^{2\times 2}$ and $G \in \mathbb{R}^{2\times 2}$ are disturbance matrices and $v_i^w(k)$ is a random vector representing exogenous gusts. When F has eigenvalues with magnitude less than one, the wind model is stable and represents a temporally correlated but bounded energy process. Spatial correlation among agents can be approximated by allowing shared components in the $v_i^w(k)$ sequences or by directly correlating the disturbance across neighboring agents. In the present linear framework, these spatial correlations can be reflected in the covariance structure without altering the basic state-space form.

To describe the swarm as a whole, it is convenient to stack the agent states into a global state vector (17). Let the number of agents be N. The global state $X(k) \in \mathbb{R}^{4N}$ and the global control $U(k) \in \mathbb{R}^{2N}$ are defined as

$$X(k) = \begin{bmatrix} x_1(k) \\ \vdots \\ (18)x_N(k) \end{bmatrix}, \quad U(k) = \begin{bmatrix} u_1(k) \\ \vdots \\ u_N(k) \end{bmatrix}. \tag{9}$$

Similarly, the global disturbance $W(k) \in \mathbb{R}^{2N}$ is

$$W(k) = (19)\begin{bmatrix} w_1(k) \\ \vdots \\ w_N(k) \end{bmatrix}. \tag{10}$$

The network dynamics can then be written as

$$X(k+1) = \mathcal{A}X(k) + \mathcal{B}U(k) + \mathcal{E}W(k), \tag{11}$$

with

$$\mathcal{A} = I_N \otimes A, \quad \mathcal{B} = I_N \otimes B, \quad \mathcal{E} = I_N \otimes E, \tag{12}$$

where $\otimes$ denotes the Kronecker product and I_N is the $N \times N$ identity matrix. This compact representation captures the fact that the agents share identical linear dynamics, while the interaction among agents enters through the choice of control law $U(k)$ (20).

The communication topology is modeled as a time-varying graph with stochastic edge activations. Let the swarm communication graph at time k be denoted by $G(k) = (V, E(k))$, where the vertex set $V = \{1, \ldots, N\}$ represents the agents and the edge set $E(k)$ describes the communication links that are successfully available at time k. For each ordered pair (i, j) with $i \neq j$, define a Bernoulli random variable $\gamma_{ij}(k)$ that takes the value 1 if agent i successfully receives a packet from agent j at time k, and 0 otherwise. These variables determine the adjacency matrix $A_c(k)$ by

$$[A_c(k)]_{ij} = \gamma_{ij}(k)a_{ij}, \tag{13}$$

where $a_{ij} \in \{0, 1\}$ is a nominal adjacency indicator that encodes the underlying communication capability, independent of instantaneous dropouts. The corresponding Laplacian matrix $L(k)$ is

$$L(k) = D(k) - A_c(k), \tag{14}$$

where $D(k)$ is the degree matrix defined by diagonal entries (21)

$$[D(k)]_{ii} = \sum_{j=1}^{N} [A_c(k)]_{ij}. \tag{15}$$

In this model, communication dropouts directly influence the Laplacian and therefore modulate the strength and structure of consensus interactions in any control law that uses neighbor information.

The stochastic variables $\gamma_{ij}(k)$ may exhibit temporal and spatial correlations depending on the physical communication medium and relative motion of agents. A common assumption for tractable analysis is that $\gamma_{ij}(k)$ are independent across pairs and time with a fixed success probability, but more general Markovian or correlated models can also be incorporated. In any case, the resulting Laplacian becomes a random matrix, and the closed-loop swarm dynamics under distributed control should be analyzed in probabilistic terms, such as mean-square stability or convergence with high probability.

Formation objectives are encoded in terms of desired relative positions (22). Let $r_i \in \mathbb{R}^2$ denote the nominal relative position of agent i with respect to a formation reference frame. The absolute desired position of agent i at time k is

$$p_i^d(k) = p_c(k) + r_i(k), \tag{16}$$

where $p_c(k) \in \mathbb{R}^2$ is a formation center or virtual leader trajectory, and $r_i(k)$ may change in time when the formation reconfigures. The reconfiguration process can be described as a sequence of desired relative patterns

$$\mathcal{R}_1, \mathcal{R}_2, \ldots, \mathcal{R}_m, \tag{17}$$

with associated sets of relative vectors $r_i^{(\ell)}$ for each pattern. Switching from one pattern to another corresponds to changing $r_i(k)$ according to a higher-level decision mechanism that may be centralized or distributed. The interaction between this pattern switching and the stochastic communication graph is central to understanding formation reconfiguration performance under realistic conditions (23).

Swarm-Intelligent Formation Reconfiguration Strategy

A swarm-intelligent formation reconfiguration strategy relies on local interaction rules that shape the global pattern

of the UAV network despite the presence of disturbances and communication imperfections. In this setting, each agent applies a control law that depends on its own state, estimates of neighbor states, and formation-related reference information. The key objective is to design interaction terms so that the swarm converges toward a desired formation pattern and performs smooth transitions when the target pattern changes, while maintaining collision avoidance and bounded control effort (*24*).

Consider the position error of agent i relative to its desired position,

$$e_i(k) = p_i(k) - p_i^d(k). \tag{18}$$

The swarm-intelligent control philosophy prescribes that the control input of agent i combines a formation tracking term based on $e_i(k)$, a consensus or alignment term based on relative positions with neighbors, and possibly a velocity damping term. Let $\mathcal{N}_i(k)$ denote the set of neighbors of agent i at time k in the nominal communication graph. Due to dropouts, agent i may only have access to a subset of these neighbors at time k. Define $\hat{p}_j^i(k)$ as the most recent position information that agent i has received from agent j. The control input is structured as (*25*)

$$u_i(k) = u_i^f(k) + u_i^c(k) + u_i^d(k), \tag{19}$$

where $u_i^f(k)$ is the formation tracking component, $u_i^c(k)$ is the consensus component, and $u_i^d(k)$ is a disturbance compensation term.

The formation tracking component can be chosen as a proportional term on the position error. A simple choice is

$$u_i^f(k) = -K_p e_i(k) - K_v v_i(k), \tag{20}$$

where $K_p \in \mathbb{R}^{2\times 2}$ and $K_v \in \mathbb{R}^{2\times 2}$ are positive definite gain matrices. This term tends to drive each agent toward its desired position while damping velocity (*26*). The consensus component aims to synchronize the agents and to maintain the relative geometry of the formation. One standard structure is

$$u_i^c(k) = -\alpha \sum_{j\in\mathcal{N}_i(k)} a_{ij}\left(\hat{p}_i^i(k) - \hat{p}_j^i(k) - \Delta_{ij}(k)\right), \tag{21}$$

where $\alpha > 0$ is a consensus gain and $\Delta_{ij}(k)$ represents the desired relative displacement between agents i and j at time k. The use of $\hat{p}_i^i(k)$ indicates that the agent uses its current estimate of its own position, which may coincide with $p_i(k)$ or a filtered version thereof. The term $\Delta_{ij}(k)$ is derived from the formation pattern and satisfies

$$\Delta_{ij}(k) = r_i(k) - r_j(k), \tag{22}$$

so that if all agents achieve $p_i(k) = p_i^d(k)$, the consensus term becomes zero.

The disturbance compensation term $u_i^d(k)$ can be based on an estimate of the wind disturbance $w_i(k)$. For linear modeling, a simple observer for $w_i(k)$ can be designed by augmenting the state with the disturbance and using a Luenberger-type structure. Let the augmented state be

$$z_i(k) = \begin{bmatrix} x_i(k) \\ w_i(k) \end{bmatrix}. \tag{23}$$

Assuming that the position $p_i(k)$ is measured, the observer can be written as

$$\hat{z}_i(k+1) = \bar{A}\hat{z}_i(k) + \bar{B}u_i(k) + L\left(y_i(k) - \hat{y}_i(k)\right), \tag{24}$$

where $y_i(k) = p_i(k)$ is the measurement, $\hat{y}_i(k)$ is the predicted output, and L is the observer gain. The matrices $\bar{A}$ and $\bar{B}$ are derived from the augmented dynamics. An estimate of the disturbance is then extracted as (*27*)

$$\hat{w}_i(k) = C_w \hat{z}_i(k), \tag{25}$$

with C_w selecting the disturbance component. The disturbance compensation term is chosen as

$$u_i^d(k) = -K_w \hat{w}_i(k), \tag{26}$$

where $K_w \in \mathbb{R}^{2\times 2}$ is a gain matrix. This term counteracts the effect of wind at the formation control level, complementing the lower-level attitude compensation.

Formation reconfiguration within this framework is implemented by changing the desired relative positions $r_i(k)$ and the associated pairwise offsets $\Delta_{ij}(k)$. A swarm-intelligent reconfiguration rule is defined by a mapping from high-level events or sensed environmental features to new formation patterns (*28*). For example, the swarm may switch from a line formation to a wedge formation when approaching an area of interest, or compress its footprint when flying through a narrow corridor. The reconfiguration can be described as a discrete event at time k_r when the reference pattern changes from $\mathcal{R}_\ell$ to $\mathcal{R}_{\ell+1}$, such that

$$r_i(k) = \begin{cases} r_i^{(\ell)}, & k < k_r, \\ r_i^{(\ell+1)}, & k \geq k_r. \end{cases} \tag{27}$$

The swarm-intelligent aspect is reflected in how agents locally interpret this change. Instead of receiving explicit new positions, agents may receive a compact description of the target pattern, such as a virtual template or shape, and perform distributed role allocation to determine individual positions (*29*).

Role allocation can be modeled as a distributed linear assignment problem, where agents iteratively adjust their target indices to minimize local cost functions. Let s_i denote the role index assigned to agent i and let q_s denote the nominal relative position associated with role s. Each agent maintains a local estimate of its role and exchanges information about its choice with neighbors. A simple cost function for agent i is (*30*)

$$J_i(s) = \|p_i(k_r) - q_s\|^2 + \beta c_i(s), \tag{28}$$

where $c_i(s)$ represents additional costs, such as fuel weight or sensing requirements, and β is a weighting factor. A distributed update rule may involve agents proposing role changes that reduce their local cost while respecting neighborhood exclusivity constraints. Although the exact assignment algorithm can be nonlinear, its effect on the formation can be captured by considering that, after convergence, each agent has a role index and a corresponding relative position vector $r_i(k)$ that defines the new pattern.

Once reconfiguration has taken place at the role level, the control law remains of the same form, but with updated reference vectors. The closed-loop dynamics during the reconfiguration transient reflect the combined effect of tracking errors, consensus interactions, and disturbance compensation (*31*). From a global linear systems perspective, the control inputs can be stacked into a global feedback law

$$U(k) = -KX(k) + HR(k) + D\hat{W}(k), \tag{29}$$

where K, H, and D are structured gain matrices derived from the local gains, $R(k)$ is the stacked vector of desired positions, and $\hat{W}(k)$ is the stacked disturbance estimate. The swarm-intelligent formation reconfiguration strategy is thus reflected in the mapping from event-driven changes in $R(k)$ to the resulting evolution of $X(k)$ under the closed-loop dynamics with stochastic communication operators.

Robust Distributed Control Under Wind and Dropouts

The presence of wind disturbances and communication dropouts necessitates the design of distributed control laws that maintain stability and acceptable performance under stochastic variations (*32*). The linear modeling developed earlier enables the treatment of these uncertainties within a unified framework. The closed-loop swarm dynamics can be expressed by combining the agent dynamics with the distributed control law in global form. Substituting the control input into the global dynamics yields (*33*)

$$X(k+1) = \mathcal{A}X(k) + \mathcal{B}U(k) + \mathcal{E}W(k). \tag{30}$$

With a linear feedback structure

$$U(k) = -KX(k) + HR(k) + D\hat{W}(k), \tag{31}$$

the closed-loop dynamics become (*34*)

$$X(k+1) = A_{cl}(k)X(k) + B_r R(k) + B_w W(k) + B_d\tilde{W}(k), \tag{32}$$

where the time dependence of $A_{cl}(k)$ stems from the stochastic communication graph. The matrices are given by

$$A_{cl}(k) = \mathcal{A} - \mathcal{B}K(k), \tag{33}$$

$$B_r = \mathcal{B}H, \quad B_w = \mathcal{E}, \quad B_d = \mathcal{B}D, \tag{34}$$

and $\tilde{W}(k)$ denotes the estimation error in the disturbance. The feedback gain $K(k)$ incorporates the Laplacian structure associated with the communication graph through consensus terms. In particular, for a purely position-based consensus interaction, the control law can be represented as (*35*)

$$U(k) = -\left(L(k) \otimes K_c\right) P(k) - \left(I_N \otimes K_p\right) E_p(k) - \left(I_N \otimes K_v\right) V(k) + \dots \tag{35}$$

where $P(k)$ and $V(k)$ are stacked position and velocity vectors, $E_p(k)$ is the stacked position error, and K_c is a consensus gain matrix. The ellipsis indicates additional disturbance compensation and reference tracking terms (*36*). The Laplacian $L(k)$ is random due to dropouts, introducing multiplicative stochasticity into the feedback gain.

Robust distributed control design can be approached by considering statistical properties of the Laplacian. Suppose that the random matrices $L(k)$ are independent and identically distributed and that their expectation exists (*37*). Define the mean Laplacian

$$\bar{L} = \mathbb{E}[L(k)]. \tag{36}$$

A nominal closed-loop system can be formed using $\bar{L}$ in place of $L(k)$, leading to a deterministic system matrix $\bar{A}_{cl}$. Stability of this nominal system is necessary but not sufficient for stability under stochastic variations. Mean-square stability can be analyzed by examining the spectral radius of appropriate lifted system matrices. For linear systems with multiplicative noise, a sufficient condition for mean-square stability is that there exists a positive definite matrix P such that (*38*)

$$\mathbb{E}\left[A_{cl}(k)^\top P A_{cl}(k)\right] - P \prec 0, (39) \tag{37}$$

where the expectation is taken over the distribution of $L(k)$. This inequality can be expanded using the statistics of the Laplacian and the structure of the gains, leading to linear matrix inequalities in the decision variables P and the gain parameters.

For tractable design, one can restrict attention to gains of the form (*40*)

$$K(k) = \left(L(k) \otimes K_c\right) + K_0, \tag{38}$$

where K_0 collects the formation tracking and velocity damping gains that do not depend on the communication graph. Under this structure, the closed-loop matrix can be decomposed into a deterministic part plus a random part proportional to the Laplacian fluctuations. Let

$$\Delta L(k) = L(k) - \bar{L}, \tag{39}$$

and write (*41*)

$$A_{cl}(k) = \bar{A}_{cl} - \left(\mathcal{B}\left(\Delta L(k) \otimes K_c\right)\right). \tag{40}$$

Assuming that the fluctuations are small in an appropriate sense, robust stability can be studied via small-gain

arguments. Introducing a matrix norm $\|\cdot\|$ and bounding the perturbation energy, a sufficient condition is (42)

$$\|\bar{A}_{cl}^{m}\| + \eta < 1, \tag{41}$$

for some integer m and a bound η representing the effect of multiplicative noise. Although such conditions may be conservative, they relate gain selection to dropout statistics (43).

An alternative design approach is based on minimizing a quadratic performance index subject to the linear dynamics with expected Laplacian. Consider a cost function of the form

$$J = \sum_{k=0}^{\infty} \mathbb{E}\left[(44)X(k)^{\top} Q X(k) + U(k)^{\top} R U(k)\right], \tag{42}$$

where $Q \succeq 0$ and $R \succ 0$ are weighting matrices. If the disturbances have finite energy and the closed-loop system is mean-square stable, this cost is finite (45). By substituting the control law and computing the expectation with respect to the dropout process, one can derive conditions for optimal gains in a linear quadratic sense. In practice, approximate solutions are obtained by replacing the random Laplacian with its mean or by employing iterative numerical methods that account for dropout probabilities in the Riccati equation.

Disturbance rejection performance is influenced by both the feedback gains and the disturbance compensation term (46). The augmented system including the disturbance estimate can be written as

$$Z(k+1) = A_z(k) Z(k) + B_z R(k) + G_z V^{w}(k), \tag{43}$$

where $Z(k)$ stacks the plant states and observer states for all agents, and $V^{w}(k)$ stacks the wind excitation processes. The matrix $A_z(k)$ is block structured, with diagonal blocks corresponding to each agent and off-diagonal blocks reflecting consensus coupling. Mean-square stability of this augmented system and bounds on the steady-state covariance of the formation error can be studied using standard linear systems tools once the statistics of $V^{w}(k)$ are specified.

The interplay between wind disturbances and communication dropouts is visible in both the stability and performance analysis (47). Stronger feedback gains may improve disturbance rejection but increase sensitivity to missing neighbor information, because aggressive consensus terms can amplify the effect of intermittent communication. Conversely, conservative consensus gains may yield robust behavior under dropouts but allow wind-induced deviations to persist longer. The linear framework makes these trade-offs explicit by relating gains, dropout probabilities, and disturbance statistics to bounds on formation error and control effort (48).

Analysis, Simulation Scenarios, and Discussion

Analytical insight into the behavior of the swarm-intelligent formation reconfiguration scheme can be obtained by studying simplified models and by examining performance metrics that capture formation accuracy, responsiveness, and robustness. One starting point is to consider small deviations around a steady formation pattern with constant wind statistics and stationary communication dropout probabilities. Under these assumptions, the formation reference $R(k)$ becomes constant, and the closed-loop dynamics of the tracking error can be linearized as a stochastic linear system with additive and multiplicative noise (2).

Define the stacked position error vector $E_p(k)$ by

$$E_p(k) = \begin{bmatrix} e_1(k) \\ \vdots \\ e_N(k) \end{bmatrix}. \tag{44}$$

Similarly, define the stacked velocity vector $V(k)$ as before. The error dynamics can be expressed in block form as

$$\begin{bmatrix} E_p(k+1) \\ V(k+1)(49) \end{bmatrix} = A_e(k) \begin{bmatrix} E_p(k) \\ V(k) \end{bmatrix} + B_e W(k) + \dots, \tag{45}$$

where the dots indicate terms involving disturbance estimates and reference changes. The matrix $A_e(k)$ depends on the control gains and the Laplacian $L(k)$. In a nominal regime without reconfiguration, and using the mean Laplacian, the expected error dynamics are governed by (50)

$$\mathbb{E}\left[\begin{bmatrix} E_p(k+1) \\ V(k+1) \end{bmatrix}\right] (51) = \bar{A}_e \mathbb{E}\left[\begin{bmatrix} E_p(k) \\ V(k) \end{bmatrix}\right] + \bar{B}_e \bar{W}, \tag{46}$$

where $\bar{W}$ represents the mean wind disturbance, which may be zero. Stability of the mean dynamics requires that the spectral radius of $\bar{A}_e$ be less than one. This condition imposes constraints on the consensus gain, formation tracking gains, and the effective coupling strength determined by the mean Laplacian (52).

Formation performance can be quantified by metrics such as the mean-square formation error, defined as

$$J_e = \lim_{k \to \infty} \mathbb{E}\left[E_p(k)^{\top} E_p(k)\right], (53) \tag{47}$$

when the limit exists. In the linear regime, J_e can be related to the solution of a Lyapunov equation involving the closed-loop system matrices and the covariance of the wind disturbance. Similarly, the average control effort can be characterized by

$$J_u = \lim_{k \to \infty} \mathbb{E}\left[(54)U(k)^{\top} U(k)\right], \tag{48}$$

which depends on the same parameters. The trade-off between J_e and J_u reflects the familiar balance between performance and energy consumption, but in this context it also interacts with dropout statistics, because higher gains increase the magnitude of control inputs when

communication is successful but may lead to larger fluctuations when packets are lost.

Formation reconfiguration introduces transient dynamics as the reference pattern changes (55). Suppose that at time k_r the desired relative positions switch from $\mathcal{R}_\ell$ to $\mathcal{R}_{\ell+1}$. The tracking error immediately after switching is

$$e_i(k_r) = p_i(k_r) - p_c(k_r) - r_i^{(\ell+1)}, \tag{49}$$

which in general is nonzero even if the swarm was perfectly aligned with $\mathcal{R}_\ell$ just before switching. The subsequent error evolution depends on both the control gains and the level of communication success. A useful performance indicator is the reconfiguration settling time, defined as the smallest $k \geq k_r$ such that

$$\mathbb{E}\left[(56)\|E_p(k)\|^2\right] \leq \epsilon, \tag{50}$$

for a given tolerance ϵ (57). Although an explicit closed-form for this quantity is generally unavailable, its dependence on gains and dropout probabilities can be explored through linear analysis and numerical simulation.

Several simulation scenarios are useful for illustrating the qualitative behavior of the proposed framework. In a first scenario, one may consider a moderate number of agents arranged in a line formation moving through a uniform crosswind (58). The wind disturbance can be modeled with a constant mean component in one direction and small random fluctuations. Communication dropouts can be represented by independent Bernoulli variables with a fixed success probability for each link. When the crosswind is present, the disturbance compensation term strives to cancel the systematic drift, while the formation tracking and consensus terms maintain the relative spacing (59). The analysis predicts that, for suitable gains, the mean formation error remains bounded and small, while the variance of the error depends on the magnitude of wind fluctuations and the dropout probability.

In a second scenario, the swarm may encounter a spatially varying wind field, such as a shear layer, where agents at different positions experience different mean wind components. This can be modeled by allowing the mean disturbance $\bar{w}_i$ to depend linearly on the position $p_i(k)$. In the linear framework, this results in an additional term in the dynamics that couples position and disturbance (60). If the variation is gradual, the consensus interactions help align the swarm by averaging out local discrepancies, but some residual deformation of the formation may occur. The disturbance compensation design can be adapted to estimate position-dependent components, or the formation pattern can be reshaped to align with the prevailing wind direction, which is an example of a swarm-intelligent reconfiguration driven by environmental sensing.

A third scenario highlights the role of communication dropouts in formation reconfiguration. Suppose that the swarm transitions from a dispersed formation to a compact formation when entering a region with obstacles that constrain the available flight corridor (61). The reconfiguration requires agents to adjust their relative positions based on updated roles and offsets. If the dropout probability increases in this region due to signal blockage, the effective connectivity of the communication graph may intermittently degrade. The analysis indicates that during intervals of poor connectivity, reconfiguration may slow down because agents receive fewer updates about neighbor states and role allocations (62). Consensus gains can be tuned to provide sufficient responsiveness while avoiding overly aggressive corrections when communication becomes available again, which could otherwise lead to oscillations.

A fourth scenario involves partial agent failures or temporary loss of agents. When one or more agents leave the formation, either intentionally or due to faults, the formation pattern needs to adapt to maintain cohesive coverage (63). In the linear framework, removal of agents can be modeled by deleting corresponding rows and columns in the Laplacian and state vectors, and by adjusting the formation pattern accordingly. The swarm-intelligent reconfiguration strategy can reassign roles among the remaining agents based on distributed criteria. The impact on formation accuracy and control effort depends on the redundancy of the original pattern and the density of the communication graph (64). Analysis of the reduced system can provide insight into how many agent losses can be tolerated before the formation loses controllability in the relevant directions.

Across these scenarios, the interaction between wind disturbances and communication dropouts is visible in the statistical properties of formation error and reconfiguration transients. When wind disturbances are small and dropouts are rare, the swarm behaves close to a deterministic linear system, and reconfigurations can be executed quickly with modest control effort (65). As wind intensity and dropout rates increase, the effective closed-loop bandwidth must be reduced to preserve stability, which lengthens reconfiguration times and increases steady-state formation error. The linear modeling approach makes it possible to express these effects in terms of eigenvalues of system matrices and covariance matrices of disturbances, thereby linking design choices directly to performance metrics.

The discussion above is based primarily on linear analysis, which is most accurate for small deviations around nominal trajectories and moderate wind conditions (66). In practice, nonlinearity in the UAV dynamics and saturation of control inputs may become significant under strong gusts or aggressive maneuvers, and these effects would need to be examined with more detailed models. Nevertheless, the linear framework provides a useful baseline for understanding how swarm-intelligent formation reconfiguration strategies interact with realistic environmental and communication uncertainties, and for guiding the selection of gains and

reference patterns that achieve desired levels of stability and robustness.

Conclusion

This article has presented a linear modeling and control framework for swarm-intelligent formation reconfiguration of UAV networks operating under wind disturbances and communication dropouts (*67*). Starting from a discrete-time double-integrator representation of individual agent dynamics with additive wind disturbances, the formulation extended to a network-level state-space model using Kronecker products. The communication structure was captured through a time-varying Laplacian matrix whose entries are modulated by stochastic packet success indicators, representing realistic wireless communication conditions. Formation objectives were encoded using desired relative positions for each agent, with reconfiguration described as event-driven changes in these relative patterns (*68*).

On the control side, a swarm-intelligent strategy was outlined in which each agent combines formation tracking, consensus-based alignment, and disturbance compensation in its local control law. This structure yields a global feedback representation in which the closed-loop system matrix depends on both consensus gains and the random communication graph. The disturbance compensation component was derived from a linear observer for the wind disturbance, enabling partial cancellation of systematic environmental effects at the formation control level (*69*). Role allocation and pattern switching were discussed in terms of distributed assignment mechanisms that map high-level formation changes into updated relative positions for individual agents.

Robust distributed control design was considered by examining mean-square stability and quadratic performance criteria under stochastic communication. The analysis emphasized how spectral properties of nominal system matrices and dropout statistics constrain the choice of feedback gains, and how wind disturbance statistics influence steady-state formation error and control effort (*70*). Sufficient conditions based on Lyapunov inequalities and approximate linear quadratic design were discussed as tools for tuning gains in the presence of multiplicative and additive uncertainties.

Finally, several representative scenarios were described to highlight the qualitative behavior of the swarm under different combinations of wind fields, dropout probabilities, and formation reconfiguration events. These scenarios illustrated the trade-offs between responsiveness and robustness, the impact of spatially varying wind on formation shape, and the effect of degraded communication on reconfiguration speed and accuracy (*71*). While the analysis relied on linear approximations and idealized disturbance models, it clarified the roles of key design parameters and provided a structured way to reason about formation performance in realistic environments.

Further work could extend the framework to include nonlinear UAV dynamics, more detailed communication models with delays and interference, and explicit collision avoidance constraints. It would also be of interest to explore adaptive and learning-based mechanisms that adjust consensus and disturbance compensation gains based on observed wind and communication conditions, while remaining compatible with the linear analysis structure where possible. Even within its linear scope, the present formulation offers a basis for systematic investigation of swarm-intelligent formation reconfiguration under combined environmental and communication uncertainties, and for comparing different distributed control strategies in a common modeling context (*72*).

References

1. null Taqdir and R. Dhir, "Hexagonal descriptor particle swarm optimization with knowledge-crowding for face recognition," *International Journal of Signal Processing, Image Processing and Pattern Recognition*, vol. 9, pp. 253–264, 9 2016.
2. G. Goggin, "Sms riot: Transmitting race on a sydney beach, december 2005: The politics of transmission," *M/C Journal*, vol. 9, 3 2006.
3. H. Kaja, R. A. Paropkari, C. Beard, and A. Van De Liefvoort, "Survivability and disaster recovery modeling of cellular networks using matrix exponential distributions," *IEEE Transactions on Network and Service Management*, vol. 18, no. 3, pp. 2812–2824, 2021.
4. B. Yigit, Y. Alapan, and M. Sitti, "Programmable collective behavior in dynamically self-assembled mobile microrobotic swarms," 1 2018.
5. K. Yeom, *ICIC (1) - Hybrid Coordinating Algorithm for Flying Robots*, pp. 140–151. Germany: Springer International Publishing, 7 2017.
6. V. Vijaykumar, R. Chandrasekar, and T. Srinivasan, "An obstacle avoidance strategy to ant colony optimization algorithm for classification in event logs," in *2006 IEEE Conference on Cybernetics and Intelligent Systems*, pp. 1–6, 2006.
7. R. Cazan, "Speaking the earth's languages: A theory for australian-chilean postcolonial poetics," *Comparative Literature Studies*, vol. 53, pp. e–1–e–5, 8 2016.
8. J. Boskovic, N. Knoebel, N. Moshtagh, J. Amin, and G. Larson, "Collaborative mission planning & autonomous control technology (compact) system employing swarms of uavs," in *AIAA Guidance, Navigation, and Control Conference*, American Institute of Aeronautics and Astronautics, 6 2009.
9. M. V. Shenoy and K. R. Anupama, "Dtta - distributed, time-division multiple access based task allocation framework for swarm robots," *Defence Science Journal*, vol. 67, pp. 316–324, 4 2017.

10. D. Gupta, A. Khanna, S. K. Lakshmanaprabu, K. Shankar, V. Furtado, and J. J. P. C. Rodrigues, "Efficient artificial fish swarm based clustering approach on mobility aware energy-efficient for manet," *Transactions on Emerging Telecommunications Technologies*, vol. 30, 11 2018.
11. P. Visu, S. Koteeswaran, and J. P. Janet, "Artificial bee colony based energy aware and energy efficient routing protocol," *Journal of Computer Science*, vol. 8, pp. 227–231, 10 2012.
12. V. R. S. M and R. Ganesan, "Bio-inspired, cluster-based deterministic node deployment in wireless sensor networks," *International Journal of Technology*, vol. 7, pp. 673–, 4 2016.
13. B. Talwar and A. K. Gupta, "Ant colony based mobile ad hoc networks routing protocols: A review," *International Journal of Computer Applications*, vol. 49, pp. 36–42, 7 2012.
14. C. Lodovisi, P. Loreti, L. Bracciale, and S. Betti, "Performance analysis of hybrid optical–acoustic auv swarms for marine monitoring," *Future Internet*, vol. 10, pp. 65–, 7 2018.
15. Z. Hasirci, I. H. Cavdar, and M. Ozturk, "Modeling and link performance analysis of busbar distribution systems for narrowband plc," *Radioengineering*, vol. 26, pp. 611–620, 6 2017.
16. T. Srinivasan, V. Vijaykumar, and R. Chandrasekar, "An auction based task allocation scheme for power-aware intrusion detection in wireless ad-hoc networks," in *2006 IFIP International Conference on Wireless and Optical Communications Networks*, pp. 5–pp, IEEE, 2006.
17. F. Schrank, "Sensor integration technologies for internet of things," *International Symposium on Microelectronics*, vol. 2015, pp. S1–S34, 10 2015.
18. H. Azami, M. Malekzadeh, S. Sanei, and A. Khosravi, "Optimization of orthogonal polyphase coding waveform for mimo radar based on evolutionary algorithms," *Journal of Mathematics and Computer Science*, vol. 06, pp. 146–153, 2 2013.
19. F. D. Rango and N. Palmieri, "Ant-based distributed protocol for coordination of a swarm of robots in demining mission," *SPIE Proceedings*, vol. 9837, pp. 983706–, 5 2016.
20. N. Deotale, U. D. Kolekar, and A. Kondelwar, "Optimal transmit antenna selection for lte system using self-adaptive grey wolf optimization," *Multiagent and Grid Systems: An International Journal of Data Science and Artificial Intelligence*, vol. 14, pp. 67–82, 2 2018.
21. F. Schlachter, C. S. F. Schwarzer, B. Girault, and P. Levi, *AMS - A Modular Software Framework for Heterogeneous Reconfigurable Robots*. Springer Berlin Heidelberg, 9 2012.
22. M. Cuibus and R. Potolea, "Wims - adaptable swarm intelligence framework," in *Proceedings of the 2nd International Conference on Web Intelligence, Mining and Semantics*, pp. 39–7, ACM, 6 2012.
23. L. Ben-Alon, R. Sacks, and Y. J. Grobman, "Similarities and differences between humans' and social insects' building processes and building behaviors," in *Construction Research Congress 2014*, pp. 51–60, American Society of Civil Engineers, 5 2014.
24. A. K. Majumdar, *Free-space Optical (FSO) Platforms: Unmanned Aerial Vehicle (UAV) and Mobile*, pp. 203–225. Germany: Springer New York, 9 2014.
25. N. Kottege and U. R. Zimmer, "Underwater acoustic localization for small submersibles," *Journal of Field Robotics*, vol. 28, pp. 40–69, 11 2010.
26. S. W. Ekanayake and P. N. Pathirana, "Formations of robotic swarm: An artificial force based approach," *International Journal of Advanced Robotic Systems*, vol. 7, pp. 7–24, 9 2010.
27. R. Chandrasekar and S. Misra, "Using zonal agent distribution effectively for routing in mobile ad hoc networks," *International Journal of Ad Hoc and Ubiquitous Computing*, vol. 3, no. 2, pp. 82–89, 2008.
28. P.-L. Buono and R. Eftimie, "Symmetries and pattern formation in hyperbolic versus parabolic models of self-organised aggregation," *Journal of mathematical biology*, vol. 71, pp. 847–881, 10 2014.
29. B. Dai, Z. Wenwen, J. Yang, and L. Lv, "Codec: Content distribution with (n,k) erasure code in manet," *International journal of Computer Networks & Communications*, vol. 6, pp. 39–51, 7 2014.
30. Y. Zhou, H. Wang, and S. Li, *CSPS - Research on the Deployment Algorithm of Distributed Detection Network*, pp. 2467–2475. Germany: Springer Singapore, 6 2018.
31. K. R. Mahmoud and A. M. Montaser, "Synthesis of multi-polarised upside conical frustum array antenna for 5g mm-wave base station at 28/38 ghz," *IET Microwaves, Antennas & Propagation*, vol. 12, pp. 1559–1569, 4 2018.
32. H. ur Rehman, S. I. Shah, I. Zaka, and J. Ahmad, "An mber–blast algorithm for ofdm–sdma communication using particle swarm optimization," *International Journal of Communication Systems*, vol. 24, pp. 185–201, 1 2011.
33. A. C. Kammara and A. König, *Advanced Methods for 3D Magnetic Localization in Industrial Process Distributed Data-Logging with a Sparse Distance Matrix*, pp. 3–13. Springer International Publishing, 11 2013.
34. M. S. Couceiro, A. Fernandes, R. P. Rocha, and N. M. F. Ferreira, "Understanding the communication complexity of the robotic darwinian pso," *Robotica*, vol. 33, pp. 157–180, 2 2014.
35. C. Röhrig, C. Kirsch, J. Lategahn, and M. Müller, *Global Localization and Position Tracking of Autonomous Transport Vehicles*, pp. 325–339. Germany: Springer Netherlands, 12 2012.
36. A. H. Ferreira and C. Martinho, "Ecal - asap: an ant resource search algorithm for swarm-like p2p networks," in *Advances in Artificial Life, ECAL 2013*, vol. 12, pp. 649–656, MIT Press, 9 2013.
37. K. Bolla, Z. C. Johanyák, T. Kovács, and G. Fazekas, *Local Center of Gravity Based Gathering Algorithm for Fat Robots*, pp. 175–183. Germany: Springer International Publishing, 1 2014.
38. T. Srinivasan, R. Chandrasekar, V. Vijaykumar, V. Mahadevan, A. Meyyappan, and M. Nivedita, "Exploring the synergism of a multiple auction-based task allocation scheme for power-aware

intrusion detection in wireless ad-hoc networks," in *2006 10th IEEE Singapore International Conference on Communication Systems*, pp. 1–5, IEEE, 2006.

39. L. Arya and S. C. Sharma, *SocProS - Coverage of Indoor WLAN in Obstructed Environment Using Particle Swarm Optimization*, pp. 1583–1594. Springer India, 2 2014.
40. J. A. Gutiérrez-Barranquero, F. J. Reen, R. R. McCarthy, A. D. W. Dobson, and F. O'Gara, "Deciphering the role of coumarin as a novel quorum sensing inhibitor suppressing virulence phenotypes in bacterial pathogens," *Applied microbiology and biotechnology*, vol. 99, pp. 3303–3316, 2 2015.
41. F. Delsuc, "Army ants trapped by their evolutionary history.," *PLoS biology*, vol. 1, pp. E37–, 11 2003.
42. K. Katayama, K.-T. Chen, and T. Baba, "Particle swarm optimization for comprehensive 24 ghz amplifier design," *Journal of Signal Processing*, vol. 22, pp. 243–250, 11 2018.
43. M. Rehman, N. Javaid, M. J. Ali, T. Saif, M. H. Ashraf, and S. H. Abbasi, *3PGCIC - Threshold Based Load Balancer for Efficient Resource Utilization of Smart Grid Using Cloud Computing*. Springer International Publishing, 10 2018.
44. R. P. S. Manikandan and A. M. Kalpana, "Feature selection using fish swarm optimization in big data," *Cluster Computing*, vol. 22, pp. 10825–10837, 9 2017.
45. S. Periyanayagi and V. Sumathy, "Swarm-based defense technique for tampering and cheating attack in wsn using cphs," *Personal and Ubiquitous Computing*, vol. 22, pp. 1165–1179, 6 2018.
46. I. R. Priyadana, B. A. A. Sumbodo, and T. W. Widodo, "Implementasi algoritma pso pada multi mobile robot dalam penentuan posisi target terdekat," *IJEIS (Indonesian Journal of Electronics and Instrumentation Systems)*, vol. 8, pp. 13–24, 4 2018.
47. A. Sekunda, M. Komareji, and R. Bouffanais, "Interplay between signaling network design and swarm dynamics," *Network Science*, vol. 4, pp. 244–265, 5 2016.
48. C. Ramachandran, S. Misra, and M. Obaidat, "On evaluating some agent-based intrusion detection schemes in mobile ad-hoc networks," in *Proceedings of the SPECTS 2007*, (San Diego, CA), pp. 594–601, July 2007.
49. R. L. M. Lee, "Do online crowds really exist? proximity, connectivity and collectivity," *Distinktion: Journal of Social Theory*, vol. 18, pp. 82–94, 8 2016.
50. G. Bonnet and C. Tessier, "Aamas - collaboration among a satellite swarm," in *Proceedings of the 6th international joint conference on Autonomous agents and multiagent systems*, pp. 54–8, ACM, 5 2007.
51. O. P. Acharya and A. Patnaik, *Particle swarm optimization for antenna array synthesis, diagnosis and healing*, pp. 495–530. Institution of Engineering and Technology, 9 2018.
52. Y. Gao, G. Zhang, J. Lu, and H.-M. Wee, "Particle swarm optimization for bi-level pricing problems in supply chains," *Journal of Global Optimization*, vol. 51, pp. 245–254, 9 2010.
53. M. Pluhacek, A. Viktorin, R. Senkerik, T. Kadavy, and I. Zelinka, "Extended experimental study on pso with partial population restart based on complex network analysis," *Logic Journal of the IGPL*, vol. 28, pp. 211–225, 10 2018.
54. T. Kuyucu, I. Tanev, and K. Shimohara, "Hormone-inspired behaviour switching for the control of collective robotic organisms," *Robotics*, vol. 2, pp. 165–184, 7 2013.
55. P. Singh, "Favorable trail detection using aco-bellman algorithm in vanets," *International Journal of Modern Education and Computer Science*, vol. 8, pp. 33–39, 1 2016.
56. K. Chen, S. Zhao, and N. Lv, "Network monitoring information collection in the sdn-enabled airborne tactical network," *International Journal of Aerospace Engineering*, vol. 2018, pp. 1–20, 9 2018.
57. V. Nagireddy, P. Parwekar, and T. K. Mishra, *Comparative Analysis of PSO-SGO Algorithms for Localization in Wireless Sensor Networks*, pp. 401–409. Springer Singapore, 12 2018.
58. R. Chandrasekar, V. Vijaykumar, and T. Srinivasan, "Probabilistic ant based clustering for distributed databases," in *2006 3rd International IEEE Conference Intelligent Systems*, pp. 538–545, IEEE, 2006.
59. R. Sinha, A. Choubey, and S. K. Mahto, "Wind driven optimization technique for equalization of non-minimum phase channel," *Indian Journal of Science and Technology*, vol. 10, pp. 1–11, 4 2017.
60. A.-D. Nguyen, P. Sénac, V. Ramiro, and M. Diaz, "Mobiwac - swarm-based intelligent routing (sir): a new approach for efficient routing in content centric delay tolerant networks," in *Proceedings of the 9th ACM international symposium on Mobility management and wireless access*, pp. 137–142, ACM, 10 2011.
61. B. Meroufel and G. Belalem, "Clustering by swarm intelligence in the ad-hoc networks," *International Journal of Applied Evolutionary Computation*, vol. 5, pp. 1–13, 7 2014.
62. T. S. Lowndes, A. B. Phillips, C. A. Harris, E. Rogers, B. Chu, and E. Popova, *TAROS - Evaluating the Capabilities of a Flight-Style Swarm AUV to Perform Emergent and Adaptive Behaviours*, pp. 237–246. Germany: Springer International Publishing, 7 2017.
63. A. Akarsu and T. Girici, "Fairness aware multiple drone base station deployment," *IET Communications*, vol. 12, pp. 425–431, 2 2018.
64. S. M. ELseuofi, "Quality of service using pso algorithm," *International Journal of Computer Science and Information Technology*, vol. 4, pp. 165–175, 2 2012.
65. J. Jordan, S. Helwig, and R. Wanka, "Gecco - social interaction in particle swarm optimization, the ranked fips, and adaptive multi-swarms," in *Proceedings of the 10th annual conference on Genetic and evolutionary computation*, pp. 49–56, ACM, 7 2008.
66. P. Rod-im, O. Duangphakdee, S. E. Radloff, C. W. W. Pirk, C. Hepburn, and R. Hepburn, "Azimuth-dependent waggle dances; flight and foraging activities of the red dwarf honeybee, apis florea fabricius (1787)," *Journal of Apicultural Research*,

vol. 54, pp. 246–254, 5 2015.
67. 8 2018.
68. M. G and S. D. A, "Twitter sentiment analysis and visualization using apache spark and elasticsearch," *International Journal of Engineering & Technology*, vol. 7, pp. 314–, 7 2018.
69. R. Chandrasekar, R. Suresh, and S. Ponnambalam, "Evaluating an obstacle avoidance strategy to ant colony optimization algorithm for classification in event logs," in *2006 International Conference on Advanced Computing and Communications*, pp. 628–629, IEEE, 2006.
70. C. Rajan and N. Shanthi, "Genetic based optimization for multicast routing algorithm for manet," *Sadhana*, vol. 40, pp. 2341–2352, 12 2015.
71. B. Lindley, L. M. y Teran-Romero, and I. B. Schwartz, "Randomly distributed delayed communication and coherent swarm patterns," 1 2012.
72. S. Xue, J. Zeng, and J. Guo, *Key Aspects of PSO-Type Swarm Robotic Search: Signals Fusion and Path Planning*. InTech, 3 2010.